

First Measurement of the $D_s^+ \rightarrow K^0 \mu^+ \nu_\mu$ Decay

M. Ablikim¹, M. N. Achasov^{4,d}, P. Adlarson⁷⁷, X. C. Ai⁸², R. Aliberti³⁶, A. Amoroso^{76A,76C}, Q. An^{73,59,b}, Y. Bai⁵⁸, O. Bakina³⁷, Y. Ban^{47,i}, H.-R. Bao⁶⁵, V. Batozskaya^{1,45}, K. Begzsuren³³, N. Berger³⁶, M. Berlowski⁴⁵, M. Bertani^{29A}, D. Bettoni^{30A}, F. Bianchi^{76A,76C}, E. Bianco^{76A,76C}, A. Bortone^{76A,76C}, I. Boyko³⁷, R. A. Briere⁵, A. Brueggemann⁷⁰, H. Cai⁷⁸, M. H. Cai^{39,l,m}, X. Cai^{1,59}, A. Calcaterra^{29A}, G. F. Cao^{1,65}, N. Cao^{1,65}, S. A. Cetin^{63A}, X. Y. Chai^{47,i}, J. F. Chang^{1,59}, G. R. Che⁴⁴, Y. Z. Che^{1,59,65}, C. H. Chen⁹, Chao Chen⁵⁶, G. Chen¹, H. S. Chen^{1,65}, H. Y. Chen²¹, M. L. Chen^{1,59,65}, S. J. Chen⁴³, S. L. Chen⁴⁶, S. M. Chen⁶², T. Chen^{1,65}, X. R. Chen^{32,65}, X. T. Chen^{1,65}, X. Y. Chen^{12,h}, Y. B. Chen^{1,59}, Y. Q. Chen³⁵, Y. Q. Chen¹⁶, Z. Chen²⁵, Z. J. Chen^{26,j}, Z. K. Chen⁶⁰, S. K. Choi¹⁰, X. Chu^{12,h}, G. Cibinetto^{30A}, F. Cossio^{76C}, J. Cottee-Meldrum⁶⁴, J. J. Cui⁵¹, H. L. Dai^{1,59}, J. P. Dai⁸⁰, A. Dbeysi¹⁹, R. E. de Boer³, D. Dedovich³⁷, C. Q. Deng⁷⁴, Z. Y. Deng¹, A. Denig³⁶, I. Denysenko³⁷, M. Destefanis^{76A,76C}, F. De Mori^{76A,76C}, B. Ding^{68,1}, X. X. Ding^{47,i}, Y. Ding⁴¹, Y. Ding³⁵, Y. Q. Ding⁴⁹, Y. X. Ding³¹, J. Dong^{1,59}, L. Y. Dong^{1,65}, M. Y. Dong^{1,59,65}, X. Dong⁷⁸, M. C. Du¹, S. X. Du⁸², S. X. Du^{12,h}, Y. Y. Duan⁵⁶, P. Egorov^{37,c}, G. F. Fan⁴³, J. J. Fan²⁰, Y. H. Fan⁴⁶, J. Fang^{1,59}, J. Fang⁶⁰, S. S. Fang^{1,65}, W. X. Fang¹, Y. Q. Fang^{1,59}, R. Farinelli^{30A}, L. Fava^{76B,76C}, F. Feldbauer³, G. Felici^{29A}, C. Q. Feng^{73,59}, J. H. Feng¹⁶, L. Feng^{39,l,m}, Q. X. Feng^{39,l,m}, Y. T. Feng^{73,59}, M. Fritsch³, C. D. Fu¹, J. L. Fu⁶⁵, Y. W. Fu^{1,65}, H. Gao⁶⁵, X. B. Gao⁴², Y. Gao^{73,59}, Y. N. Gao²⁰, Y. N. Gao^{47,i}, Y. Y. Gao³¹, S. Garbolino^{76C}, I. Garzia^{30A,30B}, L. Ge⁵⁸, P. T. Ge²⁰, Z. W. Ge⁴³, C. Geng⁶⁰, E. M. Gersabeck⁶⁹, A. Gilman⁷¹, K. Goetzen¹³, J. D. Gong³⁵, L. Gong⁴¹, W. X. Gong^{1,59}, W. Gradi³⁶, S. Gramigna^{30A,30B}, M. Greco^{76A,76C}, M. H. Gu^{1,59}, Y. T. Gu¹⁵, C. Y. Guan^{1,65}, A. Q. Guo³², L. B. Guo⁴², M. J. Guo⁵¹, R. P. Guo⁵⁰, Y. P. Guo^{12,h}, A. Guskov^{37,c}, J. Gutierrez²⁸, K. L. Han⁶⁵, T. T. Han¹, F. Hanisch³, K. D. Hao^{73,59}, X. Q. Hao²⁰, F. A. Harris⁶⁷, K. K. He⁵⁶, K. L. He^{1,65}, F. H. Heinsius³, C. H. Heinz³⁶, Y. K. Heng^{1,59,65}, C. Herold⁶¹, P. C. Hong³⁵, G. Y. Hou^{1,65}, X. T. Hou^{1,65}, Y. R. Hou⁶⁵, Z. L. Hou¹, H. M. Hu^{1,65}, J. F. Hu^{57,k}, Q. P. Hu^{73,59}, S. L. Hu^{12,h}, T. Hu^{1,59,65}, Y. Hu¹, Z. M. Hu⁶⁰, G. S. Huang^{73,59}, K. X. Huang⁶⁰, L. Q. Huang^{32,65}, P. Huang⁴³, X. T. Huang⁵¹, Y. P. Huang¹, Y. S. Huang⁶⁰, T. Hussain⁷⁵, N. Hüsken³⁶, N. in der Wiesche⁷⁰, J. Jackson²⁸, Q. Ji¹, Q. P. Ji²⁰, W. Ji^{1,65}, X. B. Ji^{1,65}, X. L. Ji^{1,59}, Y. Y. Ji⁵¹, Z. K. Jia^{73,59}, D. Jiang^{1,65}, H. B. Jiang⁷⁸, P. C. Jiang^{47,i}, S. J. Jiang⁹, T. J. Jiang¹⁷, X. S. Jiang^{1,59,65}, Y. Jiang⁶⁵, J. B. Jiao⁵¹, J. K. Jiao³⁵, Z. Jiao²⁴, S. Jin⁴³, Y. Jin⁶⁸, M. Q. Jing^{1,65}, X. M. Jing⁶⁵, T. Johansson⁷⁷, S. Kabana³⁴, N. Kalantar-Nayestanaki⁶⁶, X. L. Kang⁹, X. S. Kang⁴¹, M. Kavatsyuk⁶⁶, B. C. Ke⁸², V. Khachatryan²⁸, A. Khoukaz⁷⁰, R. Kiuchi¹, O. B. Kolcu^{63A}, B. Kopf³, M. Kuessner³, X. Kui^{1,65}, N. Kumar²⁷, A. Kupsc^{45,77}, W. Kühn³⁸, Q. Lan⁷⁴, W. N. Lan²⁰, T. T. Lei^{73,59}, M. Lellmann³⁶, T. Lenz³⁶, C. Li⁴⁸, C. Li⁴⁴, C. H. Li⁴⁰, C. K. Li²¹, D. M. Li⁸², F. Li^{1,59}, G. Li¹, H. B. Li^{1,65}, H. J. Li²⁰, H. N. Li^{57,k}, Hui Li⁴⁴, J. R. Li⁶², J. S. Li⁶⁰, K. Li¹, K. L. Li^{39,l,m}, K. L. Li²⁰, L. J. Li^{1,65}, Lei Li⁴⁹, M. H. Li⁴⁴, M. R. Li^{1,65}, P. L. Li⁶⁵, P. R. Li^{39,l,m}, Q. M. Li^{1,65}, Q. X. Li⁵¹, R. Li^{18,32}, S. X. Li¹², T. Li⁵¹, T. Y. Li⁴⁴, W. D. Li^{1,65}, W. G. Li^{1,b}, X. Li^{1,65}, X. H. Li^{73,59}, X. L. Li⁵¹, X. Y. Li^{1,8}, X. Z. Li⁶⁰, Y. Li²⁰, Y. G. Li^{47,i}, Y. P. Li³⁵, Z. J. Li⁶⁰, Z. Y. Li⁸⁰, H. Liang^{73,59}, Y. F. Liang⁵⁵, Y. T. Liang^{32,65}, G. R. Liao¹⁴, L. B. Liao⁶⁰, M. H. Liao⁶⁰, Y. P. Liao^{1,65}, J. Libby²⁷, A. Limphirat⁶¹, C. C. Lin⁵⁶, D. X. Lin^{32,65}, L. Q. Lin⁴⁰, T. Lin¹, B. J. Liu¹, B. X. Liu⁷⁸, C. Liu³⁵, C. X. Liu¹, F. Liu¹, F. H. Liu⁵⁴, Feng Liu⁶, G. M. Liu^{57,k}, H. Liu^{39,l,m}, H. B. Liu¹⁵, H. H. Liu¹, H. M. Liu^{1,65}, Huihui Liu²², J. B. Liu^{73,59}, J. J. Liu²¹, K. Liu^{39,l,m}, K. Liu⁷⁴, K. Y. Liu⁴¹, Ke Liu²³, L. C. Liu⁴⁴, Lu Liu⁴⁴, M. H. Liu^{12,h}, P. L. Liu¹, Q. Liu⁶⁵, S. B. Liu^{73,59}, T. Liu^{12,h}, W. K. Liu⁴⁴, W. M. Liu^{73,59}, W. T. Liu⁴⁰, X. Liu^{39,l,m}, X. Liu⁴⁰, X. K. Liu^{39,l,m}, X. L. Liu^{12,h}, X. Y. Liu⁷⁸, Y. Liu^{39,l,m}, Y. Liu⁸², Y. Liu⁸², Y. B. Liu⁴⁴, Z. A. Liu^{1,59,65}, Z. D. Liu⁹, Z. Q. Liu⁵¹, X. C. Lou^{1,59,65}, F. X. Lu⁶⁰, H. J. Lu²⁴, J. G. Lu^{1,59}, X. L. Lu¹⁶, Y. Lu⁷, Y. H. Lu^{1,65}, Y. P. Lu^{1,59}, Z. H. Lu^{1,65}, C. L. Luo⁴², J. R. Luo⁶⁰, J. S. Luo^{1,65}, M. X. Luo⁸¹, T. Luo^{12,h}, X. L. Luo^{1,59}, Z. Y. Lv²³, X. R. Lyu^{65,q}, Y. F. Lyu⁴⁴, Y. H. Lyu⁸², F. C. Ma⁴¹, H. L. Ma¹, J. L. Ma^{1,65}, L. L. Ma⁵¹, L. R. Ma⁶⁸, Q. M. Ma¹, R. Q. Ma^{1,65}, R. Y. Ma²⁰, T. Ma^{73,59}, X. T. Ma^{1,65}, X. Y. Ma^{1,59}, Y. M. Ma³², F. E. Maas¹⁹, I. MacKay⁷¹, M. Maggiore^{76A,76C}, S. Malde⁷¹, Q. A. Malik⁷⁵, H. X. Mao^{39,l,m}, Y. J. Mao^{47,i}, Z. P. Mao¹, S. Marcello^{76A,76C}, A. Marshall⁶⁴, F. M. Melendi^{30A,30B}, Y. H. Meng⁶⁵, Z. X. Meng⁶⁸, G. Mezzadri^{30A}, H. Miao^{1,65}, T. J. Min⁴³, R. E. Mitchell²⁸, X. H. Mo^{1,59,65}, B. Moses²⁸, N. Yu. Muchnoi^{4,d}, J. Muskalla³⁶, Y. Nefedov³⁷, F. Nerling^{19,f}, L. S. Nie²¹, I. B. Nikolaev^{4,d}, Z. Ning^{1,59}, S. Nisar^{11,n}, Q. L. Niu^{39,l,m}, W. D. Niu^{12,h}, C. Normand⁶⁴, S. L. Olsen^{10,65}, Q. Ouyang^{1,59,65}, S. Pacetti^{29B,29C}, X. Pan⁵⁶, Y. Pan⁵⁸, A. Pathak¹⁰, Y. P. Pei^{73,59}, M. Pelizaeus³, H. P. Peng^{73,59}, X. J. Peng^{39,l,m}, Y. Y. Peng^{39,l,m}, K. Peters^{13,f}, K. Petridis⁶⁴, J. L. Ping⁴², R. G. Ping^{1,65}, S. Plura³⁶, V. Prasad³⁵, F. Z. Qi¹, H. R. Qi⁶², M. Qi⁴³, S. Qian^{1,59}, W. B. Qian⁶⁵, C. F. Qiao⁶⁵, J. H. Qiao²⁰, J. J. Qin⁷⁴, J. L. Qin⁵⁶, L. Q. Qin¹⁴, L. Y. Qin^{73,59}, P. B. Qin⁷⁴, X. P. Qin^{12,h}, X. S. Qin⁵¹, Z. H. Qin^{1,59}, J. F. Qiu¹, Z. H. Qu⁷⁴, J. Rademacker⁶⁴, C. F. Redmer³⁶, A. Rivetti^{76C}, M. Rolo^{76C}, G. Rong^{1,65}, S. S. Rong^{1,65}, F. Rosini^{29B,29C}, Ch. Rosner¹⁹, M. Q. Ruan^{1,59}, N. Salone⁴⁵, A. Sarantsev^{37,e}, Y. Schelhaas³⁶, K. Schoenning⁷⁷, M. Scodeggio^{30A}, K. Y. Shan^{12,h}, W. Shan²⁵, X. Y. Shan^{73,59}, Z. J. Shang^{39,l,m}, J. F. Shangguan¹⁷, L. G. Shao^{1,65}, M. Shao^{73,59}, C. P. Shen^{12,h}, H. F. Shen^{1,8}, W. H. Shen⁶⁵, X. Y. Shen^{1,65}, B. A. Shi⁶⁵, H. Shi^{73,59}, J. L. Shi^{12,h}, J. Y. Shi¹, S. Y. Shi⁷⁴, X. Shi^{1,59}, H. L. Song^{73,59}, J. J. Song²⁰, T. Z. Song⁶⁰, W. M. Song³⁵, Y. J. Song^{12,h}, Y. X. Song^{47,i,o}, S. Sosio^{76A,76C}, S. Spataro^{76A,76C}, S. Stansilaus⁷¹, F. Stieler³⁶, S. S. Su⁴¹, Y. J. Su⁶⁵, G. B. Sun⁷⁸, G. X. Sun¹, H. Sun⁶⁵, H. K. Sun¹, J. F. Sun²⁰, K. Sun⁶², L. Sun⁷⁸, S. S. Sun^{1,65}, T. Sun^{52,g}, Y. C. Sun⁷⁸, Y. H. Sun³¹, Y. J. Sun^{73,59}, Y. Z. Sun¹, Z. Q. Sun^{1,65}, Z. T. Sun⁵¹, C. J. Tang⁵⁵, G. Y. Tang¹, J. Tang⁶⁰, J. J. Tang^{73,59}, L. F. Tang⁴⁰, Y. A. Tang⁷⁸, L. Y. Tao⁷⁴, M. Tat⁷¹, J. X. Teng^{73,59}, J. Y. Tian^{73,59}, W. H. Tian⁶⁰, Y. Tian³², Z. F. Tian⁷⁸, I. Uman^{63B}, B. Wang⁶⁰, B. Wang¹, Bo Wang^{73,59}, C. Wang^{39,l,m}, C. Wang²⁰, Cong Wang²³, D. Y. Wang^{47,i}, H. J. Wang^{39,l,m}, J. J. Wang⁷⁸, K. Wang^{1,59}, L. L. Wang¹, L. W. Wang³⁵, M. Wang^{73,59}, M. Wang⁵¹, N. Y. Wang⁶⁵, S. Wang^{12,h}, T. Wang^{12,h}, T. J. Wang⁴⁴, W. Wang⁶⁰, W. Wang⁷⁴, W. P. Wang^{36,59,73,p}, X. Wang^{47,i}, X. F. Wang^{39,l,m}, X. J. Wang⁴⁰, X. L. Wang^{12,h}, X. N. Wang^{1,65}, Y. Wang⁶²,

Y. D. Wang⁴⁶, Y. F. Wang^{1,8,65}, Y. H. Wang^{39,l,m}, Y. J. Wang^{73,59}, Y. L. Wang²⁰, Y. N. Wang⁷⁸, Y. Q. Wang¹,
 Yaqian Wang¹⁸, Yi Wang⁶², Yuan Wang^{18,32}, Z. Wang^{1,59}, Z. L. Wang⁷⁴, Z. L. Wang², Z. Q. Wang^{12,h}, Z. Y. Wang^{1,65},
 D. H. Wei¹⁴, H. R. Wei⁴⁴, F. Weidner⁷⁰, S. P. Wen¹, Y. R. Wen⁴⁰, U. Wiedner³, G. Wilkinson⁷¹, M. Wolke⁷⁷, C. Wu⁴⁰,
 J. F. Wu^{1,8}, L. H. Wu¹, L. J. Wu²⁰, L. J. Wu^{1,65}, Lianjie Wu²⁰, S. G. Wu^{1,65}, S. M. Wu⁶⁵, X. Wu^{12,h}, X. H. Wu³⁵,
 Y. J. Wu³², Z. Wu^{1,59}, L. Xia^{73,59}, X. M. Xian⁴⁰, B. H. Xiang^{1,65}, D. Xiao^{39,l,m}, G. Y. Xiao⁴³, H. Xiao⁷⁴, Y. L. Xiao^{12,h},
 Z. J. Xiao⁴², C. Xie⁴³, K. J. Xie^{1,65}, X. H. Xie^{47,i}, Y. Xie⁵¹, Y. G. Xie^{1,59}, Y. H. Xie⁶, Z. P. Xie^{73,59}, T. Y. Xing^{1,65},
 C. F. Xu^{1,65}, C. J. Xu⁶⁰, G. F. Xu¹, H. Y. Xu², H. Y. Xu^{68,2}, M. Xu^{73,59}, Q. J. Xu¹⁷, Q. N. Xu³¹, T. D. Xu⁷⁴,
 W. Xu¹, W. L. Xu⁶⁸, X. P. Xu⁵⁶, Y. Xu⁴¹, Y. Xu^{12,h}, Y. C. Xu⁷⁹, Z. S. Xu⁶⁵, F. Yan^{12,h}, H. Y. Yan⁴⁰, L. Yan^{12,h},
 W. B. Yan^{73,59}, W. C. Yan⁸², W. H. Yan⁶, W. P. Yan²⁰, X. Q. Yan^{1,65}, H. J. Yang^{52,g}, H. L. Yang³⁵, H. X. Yang¹,
 J. H. Yang⁴³, R. J. Yang²⁰, T. Yang¹, Y. Yang^{12,h}, Y. F. Yang⁴⁴, Y. H. Yang⁴³, Y. Q. Yang⁹, Y. X. Yang^{1,65}, Y. Z. Yang²⁰,
 M. Ye^{1,59}, M. H. Ye^{8,b}, Z. J. Ye^{57,k}, Junhao Yin⁴⁴, Z. Y. You⁶⁰, B. X. Yu^{1,59,65}, C. X. Yu⁴⁴, G. Yu¹³, J. S. Yu^{26,j},
 L. Q. Yu^{12,h}, M. C. Yu⁴¹, T. Yu⁷⁴, X. D. Yu^{47,i}, Y. C. Yu⁸², C. Z. Yuan^{1,65}, H. Yuan^{1,65}, J. Yuan⁴⁶, J. Yuan³⁵, L. Yuan²,
 S. C. Yuan^{1,65}, X. Q. Yuan¹, Y. Yuan^{1,65}, Z. Y. Yuan⁶⁰, C. X. Yue⁴⁰, Ying Yue²⁰, A. A. Zafar⁷⁵, S. H. Zeng⁶⁴, X. Zeng^{12,h},
 Y. Zeng^{26,j}, Y. J. Zeng⁶⁰, Y. J. Zeng^{1,65}, X. Y. Zhai³⁵, Y. H. Zhan⁶⁰, Zhang⁷¹, A. Q. Zhang^{1,65}, B. L. Zhang^{1,65},
 B. X. Zhang¹, D. H. Zhang⁴⁴, G. Y. Zhang²⁰, G. Y. Zhang^{1,65}, H. Zhang^{73,59}, H. Zhang⁸², H. C. Zhang^{1,59,65}, H. H. Zhang⁶⁰,
 H. Q. Zhang^{1,59,65}, H. R. Zhang^{73,59}, H. Y. Zhang^{1,59}, J. Zhang⁶⁰, J. Zhang⁸², J. J. Zhang⁵³, J. L. Zhang²¹, J. Q. Zhang⁴²,
 J. S. Zhang^{12,h}, J. W. Zhang^{1,59,65}, J. X. Zhang^{39,l,m}, J. Y. Zhang¹, J. Z. Zhang^{1,65}, Jianyu Zhang⁶⁵, L. M. Zhang⁶²,
 Lei Zhang⁴³, N. Zhang⁸², P. Zhang^{1,8}, Q. Zhang²⁰, Q. Y. Zhang³⁵, R. Y. Zhang^{39,l,m}, S. H. Zhang^{1,65}, Shulei Zhang^{26,j},
 X. M. Zhang¹, X. Y. Zhang⁴¹, X. Y. Zhang⁵¹, Y. Zhang⁷⁴, Y. Zhang¹, Y. T. Zhang⁸², Y. H. Zhang^{1,59}, Y. M. Zhang⁴⁰,
 Y. P. Zhang^{73,59}, Z. D. Zhang¹, Z. H. Zhang¹, Z. L. Zhang³⁵, Z. L. Zhang⁵⁶, Z. X. Zhang²⁰, Z. Y. Zhang⁴⁴, Z. Y. Zhang⁷⁸,
 Z. Z. Zhang⁴⁶, Zh. Zh. Zhang²⁰, G. Zhao¹, J. Y. Zhao^{1,65}, J. Z. Zhao^{1,59}, L. Zhao^{73,59}, L. Zhao¹, M. G. Zhao⁴⁴, N. Zhao⁸⁰,
 R. P. Zhao⁶⁵, S. J. Zhao⁸², Y. B. Zhao^{1,59}, Y. L. Zhao⁵⁶, Y. X. Zhao^{32,65}, Z. G. Zhao^{73,59}, A. Zhemchugov^{37,c}, B. Zheng⁷⁴,
 B. M. Zheng³⁵, J. P. Zheng^{1,59}, W. J. Zheng^{1,65}, X. R. Zheng²⁰, Y. H. Zheng^{55,g}, B. Zhong⁴², C. Zhong²⁰, H. Zhou^{36,51,p},
 J. Q. Zhou³⁵, J. Y. Zhou³⁵, S. Zhou⁶, X. Zhou⁷⁸, X. K. Zhou⁶, X. R. Zhou^{73,59}, X. Y. Zhou⁴⁰, Y. X. Zhou⁷⁹, Y. Z. Zhou^{12,h},
 A. N. Zhu⁶⁵, J. Zhu⁴⁴, K. Zhu¹, K. J. Zhu^{1,59,65}, K. S. Zhu^{12,h}, L. Zhu³⁵, L. X. Zhu⁶⁵, S. H. Zhu⁷², T. J. Zhu^{12,h},
 W. D. Zhu^{12,h}, W. D. Zhu⁴², W. J. Zhu¹, W. Z. Zhu²⁰, Y. C. Zhu^{73,59}, Z. A. Zhu^{1,65}, X. Y. Zhuang⁴⁴, J. H. Zou¹, J. Zu^{73,59}

(BESIII Collaboration)

¹ Institute of High Energy Physics, Beijing 100049, People's Republic of China

² Beihang University, Beijing 100191, People's Republic of China

³ Bochum Ruhr-University, D-44780 Bochum, Germany

⁴ Budker Institute of Nuclear Physics SB RAS (BINP), Novosibirsk 630090, Russia

⁵ Carnegie Mellon University, Pittsburgh, Pennsylvania 15213, USA

⁶ Central China Normal University, Wuhan 430079, People's Republic of China

⁷ Central South University, Changsha 410083, People's Republic of China

⁸ China Center of Advanced Science and Technology, Beijing 100190, People's Republic of China

⁹ China University of Geosciences, Wuhan 430074, People's Republic of China

¹⁰ Chung-Ang University, Seoul, 06974, Republic of Korea

¹¹ COMSATS University Islamabad, Lahore Campus, Defence Road, Off Raiwind Road, 54000 Lahore, Pakistan

¹² Fudan University, Shanghai 200433, People's Republic of China

¹³ GSI Helmholtzcentre for Heavy Ion Research GmbH, D-64291 Darmstadt, Germany

¹⁴ Guangxi Normal University, Guilin 541004, People's Republic of China

¹⁵ Guangxi University, Nanning 530004, People's Republic of China

¹⁶ Guangxi University of Science and Technology, Liuzhou 545006, People's Republic of China

¹⁷ Hangzhou Normal University, Hangzhou 310036, People's Republic of China

¹⁸ Hebei University, Baoding 071002, People's Republic of China

¹⁹ Helmholtz Institute Mainz, Staudinger Weg 18, D-55099 Mainz, Germany

²⁰ Henan Normal University, Xinxiang 453007, People's Republic of China

²¹ Henan University, Kaifeng 475004, People's Republic of China

²² Henan University of Science and Technology, Luoyang 471003, People's Republic of China

²³ Henan University of Technology, Zhengzhou 450001, People's Republic of China

²⁴ Huangshan College, Huangshan 245000, People's Republic of China

²⁵ Hunan Normal University, Changsha 410081, People's Republic of China

²⁶ Hunan University, Changsha 410082, People's Republic of China

²⁷ Indian Institute of Technology Madras, Chennai 600036, India

²⁸ Indiana University, Bloomington, Indiana 47405, USA

²⁹ INFN Laboratori Nazionali di Frascati, (A)INFN Laboratori Nazionali di Frascati, I-00044, Frascati, Italy;

(B)INFN Sezione di Perugia, I-06100, Perugia, Italy; (C)University of Perugia, I-06100, Perugia, Italy

³⁰ INFN Sezione di Ferrara, (A)INFN Sezione di Ferrara, I-44122, Ferrara, Italy

³¹ Inner Mongolia University, Hohhot 010021, People's Republic of China

³² Institute of Modern Physics, Lanzhou 730000, People's Republic of China

³³ Institute of Physics and Technology, Mongolian Academy of Sciences, Peace Avenue 54B, Ulaanbaatar 13330, Mongolia

³⁴ Instituto de Alta Investigación, Universidad de Tarapacá, Casilla 7D, Arica 1000000, Chile
³⁵ Jilin University, Changchun 130012, People's Republic of China
³⁶ Johannes Gutenberg University of Mainz, Johann-Joachim-Becher-Weg 45, D-55099 Mainz, Germany
³⁷ Joint Institute for Nuclear Research, 141980 Dubna, Moscow region, Russia
³⁸ Justus-Liebig-Universitaet Giessen, II. Physikalisches Institut, Heinrich-Buff-Ring 16, D-35392 Giessen, Germany
³⁹ Lanzhou University, Lanzhou 730000, People's Republic of China
⁴⁰ Liaoning Normal University, Dalian 116029, People's Republic of China
⁴¹ Liaoning University, Shenyang 110036, People's Republic of China
⁴² Nanjing Normal University, Nanjing 210023, People's Republic of China
⁴³ Nanjing University, Nanjing 210093, People's Republic of China
⁴⁴ Nankai University, Tianjin 300071, People's Republic of China
⁴⁵ National Centre for Nuclear Research, Warsaw 02-093, Poland
⁴⁶ North China Electric Power University, Beijing 102206, People's Republic of China
⁴⁷ Peking University, Beijing 100871, People's Republic of China
⁴⁸ Qufu Normal University, Qufu 273165, People's Republic of China
⁴⁹ Renmin University of China, Beijing 100872, People's Republic of China
⁵⁰ Shandong Normal University, Jinan 250014, People's Republic of China
⁵¹ Shandong University, Jinan 250100, People's Republic of China
⁵² Shanghai Jiao Tong University, Shanghai 200240, People's Republic of China
⁵³ Shanxi Normal University, Linfen 041004, People's Republic of China
⁵⁴ Shanxi University, Taiyuan 030006, People's Republic of China
⁵⁵ Sichuan University, Chengdu 610064, People's Republic of China
⁵⁶ Soochow University, Suzhou 215006, People's Republic of China
⁵⁷ South China Normal University, Guangzhou 510006, People's Republic of China
⁵⁸ Southeast University, Nanjing 211100, People's Republic of China
⁵⁹ State Key Laboratory of Particle Detection and Electronics, Beijing 100049, Hefei 230026, People's Republic of China
⁶⁰ Sun Yat-Sen University, Guangzhou 510275, People's Republic of China
⁶¹ Suranaree University of Technology, University Avenue 111, Nakhon Ratchasima 30000, Thailand
⁶² Tsinghua University, Beijing 100084, People's Republic of China
⁶³ Turkish Accelerator Center Particle Factory Group, (A)Istinye University, 34010, Istanbul, Turkey; (B)Near East University, Nicosia, North Cyprus, 99138, Mersin 10, Turkey
⁶⁴ University of Bristol, H H Wills Physics Laboratory, Tyndall Avenue, Bristol, BS8 1TL, UK
⁶⁵ University of Chinese Academy of Sciences, Beijing 100049, People's Republic of China
⁶⁶ University of Groningen, NL-9747 AA Groningen, The Netherlands
⁶⁷ University of Hawaii, Honolulu, Hawaii 96822, USA
⁶⁸ University of Jinan, Jinan 250022, People's Republic of China
⁶⁹ University of Manchester, Oxford Road, Manchester, M13 9PL, United Kingdom
⁷⁰ University of Muenster, Wilhelm-Klemm-Strasse 9, 48149 Muenster, Germany
⁷¹ University of Oxford, Keble Road, Oxford OX13RH, United Kingdom
⁷² University of Science and Technology Liaoning, Anshan 114051, People's Republic of China
⁷³ University of Science and Technology of China, Hefei 230026, People's Republic of China
⁷⁴ University of South China, Hengyang 421001, People's Republic of China
⁷⁵ University of the Punjab, Lahore-54590, Pakistan
⁷⁶ University of Turin and INFN, (A)University of Turin, I-10125, Turin, Italy; (B)University of Eastern Piedmont, I-15121, Alessandria, Italy; (C)INFN, I-10125, Turin, Italy
⁷⁷ Uppsala University, Box 516, SE-75120 Uppsala, Sweden
⁷⁸ Wuhan University, Wuhan 430072, People's Republic of China
⁷⁹ Yantai University, Yantai 264005, People's Republic of China
⁸⁰ Yunnan University, Kunming 650500, People's Republic of China
⁸¹ Zhejiang University, Hangzhou 310027, People's Republic of China
⁸² Zhengzhou University, Zhengzhou 450001, People's Republic of China

^b Deceased

^c Also at the Moscow Institute of Physics and Technology, Moscow 141700, Russia
^d Also at the Novosibirsk State University, Novosibirsk, 630090, Russia
^e Also at the NRC "Kurchatov Institute", PNPI, 188300, Gatchina, Russia
^f Also at Goethe University Frankfurt, 60323 Frankfurt am Main, Germany

^g Also at Key Laboratory for Particle Physics, Astrophysics and Cosmology, Ministry of Education; Shanghai Key Laboratory for Particle Physics and Cosmology; Institute of Nuclear and Particle Physics, Shanghai 200240, People's Republic of China

^h Also at Key Laboratory of Nuclear Physics and Ion-beam Application (MOE) and Institute of Modern Physics, Fudan University, Shanghai 200443, People's Republic of China

ⁱ Also at State Key Laboratory of Nuclear Physics and Technology, Peking University, Beijing 100871, People's Republic of China

^j Also at School of Physics and Electronics, Hunan University, Changsha 410082, China

^k Also at *Guangdong Provincial Key Laboratory of Nuclear Science, Institute of Quantum Matter, South China Normal University, Guangzhou 510006, China*

^l Also at *MOE Frontiers Science Center for Rare Isotopes, Lanzhou University, Lanzhou 730000, People's Republic of China*

^m Also at *Lanzhou Center for Theoretical Physics, Lanzhou University, Lanzhou 730000, People's Republic of China*

ⁿ Also at *the Department of Mathematical Sciences, IBA, Karachi 75270, Pakistan*

^o Also at *Ecole Polytechnique Federale de Lausanne (EPFL), CH-1015 Lausanne, Switzerland*

^p Also at *Helmholtz Institute Mainz, Staudinger Weg 18, D-55099 Mainz, Germany*

^q Also at *Hangzhou Institute for Advanced Study, University of Chinese Academy of Sciences, Hangzhou 310024, China*

We report the first measurement of the semileptonic decay $D_s^+ \rightarrow K^0 \mu^+ \nu_\mu$, using a sample of $e^+ e^-$ annihilation data corresponding to an integrated luminosity of 7.33 fb^{-1} collected at center-of-mass energies between 4.128 to 4.226 GeV with the BESIII detector at the BEPCII collider. The branching fraction of the decay is measured to be $\mathcal{B}(D_s^+ \rightarrow K^0 \mu^+ \nu_\mu) = (2.89 \pm 0.27_{\text{stat}} \pm 0.12_{\text{syst}}) \times 10^{-3}$, where the first uncertainty is statistical and the second is systematic. Based on a simultaneous fit to the partial decay rates in q^2 intervals measured in $D_s^+ \rightarrow K^0 \mu^+ \nu_\mu$ and $D_s^+ \rightarrow K^0 e^+ \nu_e$ decays, the product value of the form factor $f_+^{K^0}(0)$ and the Cabibbo-Kobayashi-Maskawa matrix element $|V_{cd}|$ is measured to be $f_+^{K^0}(0)|V_{cd}| = 0.140 \pm 0.008_{\text{stat}} \pm 0.002_{\text{syst}}$. Using $|V_{cd}| = 0.22486 \pm 0.00068$ as an input, the hadronic form factor is determined to be $f_+^{K^0}(0) = 0.623 \pm 0.036_{\text{stat}} \pm 0.009_{\text{syst}}$ at $q^2 = 0$. This is the most precise determination of $f_+^{K^0}(0)$ in the $D_s^+ \rightarrow K^0$ transition to date. The measured branching fraction and form factor presented in this work provide the most stringent test on various non-perturbative theoretical calculations. Taking $f_+^{K^0}(0) = 0.6307 \pm 0.0020$ from lattice calculations as an input, we obtain $|V_{cd}| = 0.220 \pm 0.013_{\text{stat}} \pm 0.003_{\text{syst}} \pm 0.001_{\text{LQCD}}$, which is the most precise determination of $|V_{cd}|$ using the $D_s^+ \rightarrow K^0 \ell^+ \nu_\ell$ decays. In addition, lepton flavor universality is tested for the first time with $D_s^+ \rightarrow K^0 \ell^+ \nu_\ell$ decays in full and separate q^2 intervals. No obvious violation is found.

In the standard model (SM), the semileptonic (SL) decays of D_s^+ mesons provide valuable information on the weak and strong interactions within hadrons composed of heavy quarks [1, 2]. The partial decay rate is related to the product of hadronic form factor (FF) describing the strong interaction in the initial and final hadrons, and the Cabibbo-Kobayashi-Maskawa (CKM) matrix [3] element $|V_{cs(d)}|$ parametrizing the mixing between different flavors of quarks in the weak interaction. Therefore, the SL decay of D_s^+ mesons both allow determination of the CKM matrix element and provide rigorous tests on various nonperturbative theoretical calculations. In recent years, there has been a great deal of attention on the experimental studies of hadronic FFs in $D_s^+ \rightarrow P \ell^+ \nu_\ell$ decays [4], where P and ℓ refer to a pseudoscalar meson and a lepton, respectively. In particular, for $D_s^+ \rightarrow K^0$ transition, only $D_s^+ \rightarrow K^0 e^+ \nu_e$ has been experimentally reported [5, 6]. The SL decay $D_s^+ \rightarrow K^0 \mu^+ \nu_\mu$ plays an important role in understanding the $D_s^+ \rightarrow K^0$ transition. However, no such measurement has been available to date. It is also found that there is roughly 2σ tensions between the $|V_{cd}|$ extracted in the $D_s^+ \rightarrow K^0 e^+ \nu_e$ decay and that in the $D \rightarrow \pi \ell \nu_\ell$ decays [7]. Studying the dynamics in the $D_s^+ \rightarrow K^0 \mu^+ \nu_\mu$ decay will provide the necessary data to improve the precision of measuring $|V_{cd}|$ and help clarify the tension.

Theoretical calculations on FFs in $D_s^+ \rightarrow K^0$ transition are extensively carried out by a series of nonperturbative approaches [7–18], which are important in understanding the quantum-chromodynamics (QCD) theory in the charm sector. However, calculations referring to the value of FF at $q^2 = 0$, $f_+^{K^0}(0)$, differ significantly and vary in the range from $0.57 - 0.82$ [7–18].

In particular, a recent calculation using Lattice QCD show $f_+^{K^0}(0) = 0.6307(20)$ [7] in $D_s^+ \rightarrow K^0$ transitions. LQCD [19] also predicts that FFs have minimal dependence on the spectator-quark mass, with FF values in $D_s^+ \rightarrow K^0$ and $D^+ \rightarrow \pi^0$ transitions differing by less than 5%. The verification of the LQCD FF predictions at the few percent level in SL charm decays will be helpful for further applying the LQCD to SL B decays for precise determination of CKM matrix elements $|V_{cb}|$ and $|V_{ub}|$ [19–21]. However, the precision of available FF measurement serving for these tests is still very limited.

The SL decays of $D_s^+ \rightarrow K^0 \ell^+ \nu_\ell$ also offer an excellent opportunity to test lepton flavor universality (LFU) predicted by the SM [22, 23]. It is suggested that the observable LFU violation effects might appear in the SL decays mediated via $c \rightarrow d \ell^+ \nu_\ell$ [24]. In recent years, a great deal of theoretical models calculated the branching fraction (BF) of $D_s^+ \rightarrow K^0 \mu^+ \nu_\mu$ and the ratio $R_{K^0}^{\mu/e} = \frac{\mathcal{B}(D_s^+ \rightarrow K^0 \mu^+ \nu_\mu)}{\mathcal{B}(D_s^+ \rightarrow K^0 e^+ \nu_e)}$ between μ and e modes. However, significant differences among theoretical calculations are observed with the predicted BF varying in the range $(0.20 - 0.39)\%$ [8–17], and the $R_{K^0}^{\mu/e}$ in $0.96 - 1.00$ [8–17]. Hence it is important to measure the BF of $D_s^+ \rightarrow K^0 \mu^+ \nu_\mu$ and $R_{K^0}^{\mu/e}$ to distinguish among these theories and also test $\mu - e$ LFU.

In this Letter, we report the first study of the $D_s^+ \rightarrow K^0 \mu^+ \nu_\mu$ decay, including a measurement of the absolute BF, the determination of the FF and the CKM element $|V_{cd}|$, as well as a LFU test via $D_s^+ \rightarrow K^0 \ell^+ \nu_\ell$ decays. Throughout this paper, the charge-conjugate modes are implied unless explicitly noted. These measurements are performed using an $e^+ e^-$ annihilation data sample cor-

responding to an integrated luminosity of 7.33 fb^{-1} produced at center-of-mass energies between $\sqrt{s} = 4.128$ and 4.226 GeV with the BEPCII collider and collected by the BESIII detector [25, 26].

Monte Carlo (MC) simulated data samples produced with a GEANT4-based [27] software package, which includes the geometric description of the BESIII detector and the detector response, are used to determine detection efficiencies and to estimate backgrounds. The inclusive MC sample includes the production of open charm processes, the initial state radiation (ISR) production of vector charmonium(-like) states, and the continuum processes incorporated in KKMC [28]. All particle decays are modeled with EVTGEN [29] using branching fractions either taken from the Particle Data Group [4], when available, or otherwise estimated with LUNDCHARM [30]. Final state radiation (FSR) from charged final state particles is incorporated using the PHOTOS package [31]. The generation of signal $D_s^+ \rightarrow K^0 \mu^+ \nu_\mu$ incorporates knowledge of the FFs (using the z -series expansion model as mentioned below) obtained in this work.

The analysis presented in this analysis exploits the production of D_s mesons in $e^+e^- \rightarrow D_s^{*+}D_s^- + c.c.$ and uses both “single-tag” (ST) and “double-tag” (DT) samples of D_s decays [5, 6]. The STs are D_s^- mesons reconstructed from their daughter particles in one of fourteen hadronic decays as shown in Fig. 1, while the DTs are events with a ST and a D_s^+ meson reconstructed as $D_s^+ \rightarrow K^0\mu^+\nu_\mu$, with K^0 reconstructed via the $K^0 \rightarrow K_S^0 \rightarrow \pi^+\pi^-$ decay. The BF for the SL decay is given by [32, 33]

$$\mathcal{B}_{\text{SL}} = \frac{N_{\text{DT}}}{\sum_i N_{\text{ST}}^i (\epsilon_{\text{DT}}^i / \epsilon_{\text{ST}}^i)} = \frac{N_{\text{DT}}}{N_{\text{ST}} \epsilon_{\text{SL}}}, \quad (1)$$

where N_{DT} is the total yield of DT events, N_{ST} is the total ST yield, and $\epsilon_{SL} = (\sum_i N_{ST}^i \times \epsilon_{DT}^i / \epsilon_{ST}^i) / \sum_i N_{ST}^i$ is the average efficiency of reconstructing the SL decay in an ST event, weighted by the measured yields of tag modes in the data. Here, ϵ_{ST}^i and ϵ_{DT}^i are the efficiencies for finding the ST and the SL decay in the i -th tag mode, respectively.

A detailed description of the selection criteria for π^\pm , K^\pm and γ candidates is given in Refs. [32, 33]. The π^0 , η , K_S^0 , ρ^- , η and η' mesons are reconstructed using the same technique as described in Ref. [6]. For all events passing the ST selection criteria, we calculate the recoil mass against the tag with the following formula

$$M_{\text{rec}} = \sqrt{(\sqrt{s} - \sqrt{|\vec{p}_{D_s^-}|^2 + m_{D_s^-}^2})^2 - |\vec{p}_{D_s^-}|^2},$$

where m_{D_s} and $\vec{p}_{D_s^-}$ are the known mass [4] and measured momentum of the tag D_s^- . In case of multiple candidates, only the candidate with M_{rec} closest to the known D_s^{*+} mass [4] is retained. To suppress other hadronic backgrounds from non- $D_s D_s^*$ processes, requirements on the kinematic variable $M_{\text{BC}} = \sqrt{(\sqrt{s}/2)^2 - |\vec{p}_{D_s^-}|^2}$ are applied. The detailed requirements on M_{BC} are described in Ref. [6], and they are

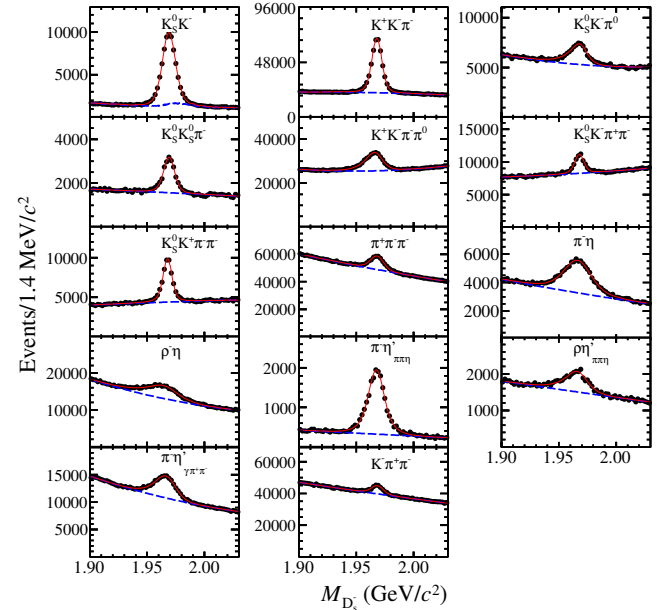


FIG. 1. (Color online) Fits to $M_{D_s^-}$ distributions for the fourteen tag modes. Points with error bars are data, blue dashed curves are the fitted backgrounds and red solid curves are the total fits.

chosen such that the tag D_s can come either directly from the production or from the $D_s^* \rightarrow D_s \gamma$ decay. To determine the mode-by-mode ST yields, we perform unbinned maximum likelihood fits to the distributions of the D_s^- invariant mass $M_{D_s^-}$, as shown in Fig. 1. Signals are modeled with the MC-derived signal shape convolved with a Gaussian function to account for the resolution differences between data and MC, while the combinatorial backgrounds are parameterized with second-order polynomial functions. Due to misidentification of π^- as K^- , the backgrounds from $D^- \rightarrow K_S^0 \pi^-$ form a broad peak near the D_s^- known mass for $D_s^- \rightarrow K_S^0 K^-$. In the fit, the shape of this background is described using MC simulation, and its size relative to other combinatorial backgrounds is fixed. For each tag mode, the ST yield is obtained by integrating the signal function over the D_s^- signal region specified by $1.94 < M_{D_s^-} < 1.99 \text{ GeV}/c^2$. The total ST yield summed over all fourteen ST modes is $N_{\text{ST}} = (783.1 \pm 2.5) \times 10^3$, where the uncertainty is statistical only.

Candidates for the SL decay $D_s^+ \rightarrow K^0 \mu^+ \nu_\mu$ are selected from the remaining tracks recoiling against the ST D_s^- mesons. The \bar{K}^0 meson is reconstructed as a $K_S^0 \rightarrow \pi^+ \pi^-$ decay with the same selection criteria as on the ST side. Apart from the two charged tracks originating from K_S^0 decays, it is required that there be only one additional track with charge opposite to the tagged D_s^- meson. For muon identification, the dE/dx and TOF measurements are combined with shower properties from the electromagnetic calorimeter (EMC) to construct likelihoods for the electron, muon, and kaon hypotheses, \mathcal{L}_e ,

\mathcal{L}_μ , and \mathcal{L}_K , respectively. The muon candidate must satisfy $\mathcal{L}_\mu > 0.001$, $\mathcal{L}_\mu > \mathcal{L}_e$, and $\mathcal{L}_\mu > \mathcal{L}_K$. Additionally, the deposited EMC energy (EMC_μ) of the muon candidate is required to be within $0.1 < \text{EMC}_\mu < 0.3$ GeV. The background from $D_s^+ \rightarrow K^0\pi^+$ decay reconstructed as $D_s^+ \rightarrow K^0\mu^+\nu_\mu$ is rejected by requiring the $K^0\mu^+$ invariant mass ($M_{K^0\mu^+}$) to be less than 1.70 GeV/ c^2 . Backgrounds containing additional π^0 mesons are further suppressed by requiring the maximum energy of any unused photon ($E_{\gamma\text{max}}$) to be less than 0.15 GeV.

To identify a photon produced directly from $D_s^{*\pm}$, a kinematic fit is performed by requiring the $D_s^\mp D_s^{*\pm}$ pair to conserve energy and momentum in the center-of-mass frame [5], and the resultant χ^2 is required to satisfy $\chi^2 < 40$. We obtain information about the undetected neutrino with the missing-mass squared of an event, calculated by the energies and momenta of the tag ($E_{D_s^-}$, $\vec{p}_{D_s^-}$), transition photon (E_γ , \vec{p}_γ), and the detected SL products ($E_{\text{SL}} = E_{K^0} + E_{\mu^+}$, $\vec{p}_{\text{SL}} = \vec{p}_{K^0} + \vec{p}_{\mu^+}$) by

$$\text{MM}^2 = (\sqrt{s} - E_{D_s^-} - E_\gamma - E_{\text{SL}})^2 - (|\vec{p}_{D_s^-} + \vec{p}_\gamma + \vec{p}_{\text{SL}}|)^2.$$

Figure 2 shows the MM^2 distribution of the accepted candidate events for $D_s^+ \rightarrow K^0\mu^+\nu_\mu$ in data. The signal DT yield N_{DT} is obtained by performing an unbinned maximum likelihood fit to MM^2 . In the fit, the signal is described with an MC-derived signal shape convolved with a Gaussian, and the combinatorial background is described by a shape obtained from the inclusive MC sample. The residual peaking background from $D_s^+ \rightarrow K^0\pi^+\pi^0$ is simulated using the MC-derived shape, with its yield fixed to 27.2 based on the MC simulation. We obtain $N_{\text{DT}} = 147.1 \pm 13.9$ events for $D_s^+ \rightarrow K^0\mu^+\nu_\mu$, where the uncertainties are statistical only. No peaking backgrounds are observed in the K^0 mass sidebands. The average efficiency of reconstructing the SL decay ϵ_{SL} is estimated to be $(18.78 \pm 0.02)\%$, where the BF of $K^0 \rightarrow \pi^+\pi^-$ is not included [34]. The BF of $D_s^+ \rightarrow K^0\mu^+\nu_\mu$ is determined by Eq. (1), and we obtain $\mathcal{B}(D_s^+ \rightarrow K^0\mu^+\nu_\mu) = (2.89 \pm 0.27) \times 10^{-3}$, where the uncertainty is statistical only.

With the DT technique, the BF measurements are insensitive to the systematic uncertainties of the ST selection. The uncertainties of the μ^+ tracking and PID efficiency is 1.0% each studied with $e^+e^- \rightarrow \gamma\mu^+\mu^-$ events, while the uncertainty due to the K^0 reconstruction is 1.5% using the control samples $J/\psi \rightarrow K^*\mp K^\pm$ and $J/\psi \rightarrow \phi K^0 K^\pm \pi^\mp$. The uncertainty associated with the MM^2 fit is estimated to be 1.2% by varying the fit ranges, the signal and the background shapes. The uncertainty due to the selection of the γ is estimated to be 1.0% based on selecting the best photon candidate in a control sample of $e^+e^- \rightarrow D_s^{*\pm} \bar{D}_s^\mp$ events with two hadronic tags, $D_s^+ \rightarrow K_S^0 K^+$ and $D_s^+ \rightarrow K^+ K^- \pi^+$. The systematic uncertainties due to the requirements of $E_{\gamma\text{max}}$ and χ^2 are estimated using the control samples $D_s^+ \rightarrow K_S^0 K^+$ and $D_s^+ \rightarrow K_S^0 K^+ \pi^0$. The differences of the acceptance efficiencies between data and MC simu-

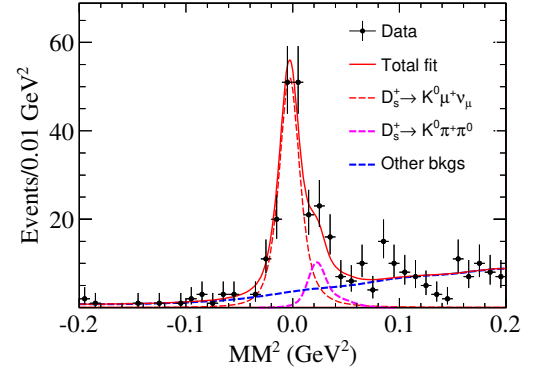


FIG. 2. (Color online) Fits to the MM^2 distribution of SL candidate events. Dots with error bars are data, dot-dashed lines (blue) are the fitted combinatorial backgrounds and solid curves (red) are the total fits. The long-dashed lines (pink) show the fitted background from $D_s^+ \rightarrow K^0\pi^+\pi^0$.

lation, 1.7% and 2.0%, are assigned as their systematic uncertainties. The uncertainties due to the $M_{K^0\mu^+}$ requirement is estimated to be 1.1% by comparing the nominal BF with that measured with alternative requirement. The uncertainty due to the MC signal modeling is estimated to be 0.9% by varying the input FF parameter by $\pm 1\sigma$ measured in this work. We also consider the systematic uncertainties of N_{ST} (1.0%), evaluated by using alternative signal shapes when fitting the $M_{D_s^-}$ spectra, the quoted BF for $K_S^0 \rightarrow \pi^+\pi^-$ (0.2%), and the MC statistics (0.8%). The uncertainty due to different tag dependencies between data and MC simulation is estimated to be 0.2%. Adding these contributions in quadrature gives total systematic uncertainty of 4.2% for the BF measurement. Finally, we determine the BF to be $\mathcal{B}(D_s^+ \rightarrow K^0\mu^+\nu_\mu) = (2.89 \pm 0.27_{\text{stat}} \pm 0.12_{\text{syst}}) \times 10^{-3}$.

To improve the experimental precision of the FF parameter in the $D_s^+ \rightarrow K^0$ transition, the candidates from $D_s^+ \rightarrow K^0\mu^+\nu_\mu$ and $D_s^+ \rightarrow K^0e^+\nu_e$ are analyzed simultaneously. The candidates of $D_s^+ \rightarrow K^0e^+\nu_e$ are selected as in Ref. [6]. The partial decay rate of $D_s^+ \rightarrow K^0\ell^+\nu_\ell$ is measured by analyzing the $\ell^+\nu_\ell$ mass-squared (q^2) distribution. The q^2 distributions of $D_s^+ \rightarrow K^0\ell^+\nu_\ell$ candidates are divided into seven bins, $[m_\ell^2, 0.35]$, $[0.35, 0.70]$, $[0.70, 1.05]$, $[1.05, 1.40]$ and $[1.40, q_{\text{max}}^2]$ GeV $^2/c^4$, where $q_{\text{max}}^2 = (m_{D_s} - m_\ell)^2$ and m_ℓ is the known mass of the lepton [4]. The measured partial decay rate in the i -th q^2 bin, $\Delta\Gamma_{\text{meas}}^i$, is determined by

$$\Delta\Gamma_{\text{meas}}^i = \sum_{j=1}^{N_{\text{bins}}} (\epsilon^{-1})_{ij} N_{\text{DT}}^j / (\tau_{D_s} \times N_{\text{ST}}),$$

where $\tau_{D_s} = (501.2 \pm 2.2)$ fs is the lifetime of D_s^+ [4] and ϵ_{ij} is an efficiency matrix to describe the reconstruction efficiency of SL decays and migration effects across q^2 bins [35, 36]. The SL signal yield observed in the j -th q^2 bin, N_{DT}^j , is obtained from a fit to the correspond-

TABLE I. The measured partial decay rates for SL decays of $D_s^+ \rightarrow K^0 \ell^+ \nu_\ell$ in various q^2 bins, where the uncertainties are statistical only [37]. The systematic uncertainties of measuring $\Delta\Gamma_{K^0 \mu^+ \nu_\mu}^i$ ($\Delta\Gamma_{K^0 e^+ \nu_e}^i$) from lower to higher q^2 intervals are 4.2 (3.9)%, 4.3 (4.0)%, 4.4 (4.5)%, 4.2 (3.8) %, and 5.3 (6.0)%, respectively.

q^2 interval	$\Delta\Gamma_{K^0 \mu^+ \nu_\mu}^i$ (ns $^{-1}$)	$\Delta\Gamma_{K^0 e^+ \nu_e}^i$ (ns $^{-1}$)	$\frac{\Delta\Gamma_{K^0 \mu^+ \nu_\mu}^i}{\Delta q^2}$ (ns $^{-1}$ GeV $^{-2}$)	$\frac{\Delta\Gamma_{K^0 e^+ \nu_e}^i}{\Delta q^2}$ (ns $^{-1}$ GeV $^{-2}$)
$[m_\ell^2, 0.35]$	1.57 ± 0.31	1.63 ± 0.24	4.62 ± 0.90	4.65 ± 0.68
$[0.35, 0.70]$	1.09 ± 0.24	1.27 ± 0.22	3.12 ± 0.66	3.62 ± 0.62
$[0.70, 1.05]$	0.93 ± 0.23	1.18 ± 0.21	2.65 ± 0.62	3.38 ± 0.61
$[1.05, 1.40]$	1.24 ± 0.25	1.08 ± 0.19	3.55 ± 0.70	3.08 ± 0.56
$[1.40, q_{\max}^2]$	0.97 ± 0.23	0.84 ± 0.19	1.27 ± 0.30	1.10 ± 0.24

ing MM 2 distribution. The measured partial decay rates $\Delta\Gamma_{\text{meas}}^i$, and the differential decay rates, $\Delta\Gamma_{\text{meas}}^i/\Delta q^2$, for SL decays $D_s^+ \rightarrow K^0 \mu^+ \nu_\mu$ and $D_s^+ \rightarrow K^0 e^+ \nu_e$, are summarized in Table I.

The expected differential decay rate in $D_s^+ \rightarrow K^0 \ell^+ \nu_\ell$ with respect to q^2 is expressed as [17]

$$\frac{d\Gamma^{\text{exp}}}{dq^2} = \frac{G_F^2 |V_{cd}|^2 |\vec{p}_{K^0}|^2}{96\pi^3 m_{D_s}^2} \lambda \left(1 - \frac{m_\ell^2}{q^2}\right)^2 |f_+^{K^0}(q^2)|^2 \left(1 + \frac{m_\ell^2}{2q^2}\right), \quad (2)$$

where G_F is the Fermi coupling constant, $\lambda = m_{D_s}^4 + m_{K^0}^4 + q^4 - 2(m_{D_s}^2 m_{K^0}^2 + m_{K^0}^2 q^2 + m_{D_s}^2 q^2)$, $|\vec{p}_{K^0}| = \lambda^{1/2}/(2m_{D_s})$ is the momentum of K^0 in the D_s^+ rest frame, m_{K^0} is the known mass of K^0 meson [4], and the $f_+^{K^0}(q^2)$ is the hadronic FF in $D_s^+ \rightarrow K^0$ transition.

To extract the FF parameter, a least- χ^2 fit is performed to the measured $\Delta\Gamma_{\text{meas}}^i$, and the theoretically expected $\Delta\Gamma_{\text{exp}}^i$, partial decay rates among q^2 intervals. The FF $f_+^{K^0}(q^2)$ in Eq. (2) is expressed using three theoretical parameterizations, which are the simple pole and modified pole models [38], as well as the z -series expansion [39]. Taking into account the correlations of the measured partial decay rates among q^2 bins, the χ^2 to be minimized is defined by

$$\chi^2 = \sum_{i,j=1}^5 (\Delta\Gamma_{\text{meas}}^i - \Delta\Gamma_{\text{exp}}^i) C_{ij}^{-1} (\Delta\Gamma_{\text{meas}}^j - \Delta\Gamma_{\text{exp}}^j), \quad (3)$$

where $C_{ij} = C_{ij}^{\text{stat}} + C_{ij}^{\text{syst}}$ is the covariance matrix of the measured partial decay rates among q^2 intervals. The statistical covariance matrix is constructed as $C_{ij}^{\text{stat}} = (\frac{1}{\tau_{D_s} \cdot N_{\text{ST}}})^2 \sum_\alpha \varepsilon_{i\alpha}^{-1} \varepsilon_{j\alpha}^{-1} [\sigma(N_{\text{DT}}^\alpha)]^2$, where α labels the q^2 interval, and $\sigma(N_{\text{DT}}^\alpha)$ is the statistical uncertainty of DT yield observed in the α^{th} q^2 interval. The systematic covariance matrix is obtained by summing over the covariance matrix of each systematic uncertainty source, which takes the form as $C_{ij}^{\text{syst}} = \delta(\Delta\Gamma_{\text{meas}}^i) \delta(\Delta\Gamma_{\text{meas}}^j)$, where $\delta(\Delta\Gamma_{\text{meas}}^i)$ is the systematic uncertainty of the measured partial decay rate in the i^{th} q^2 interval.

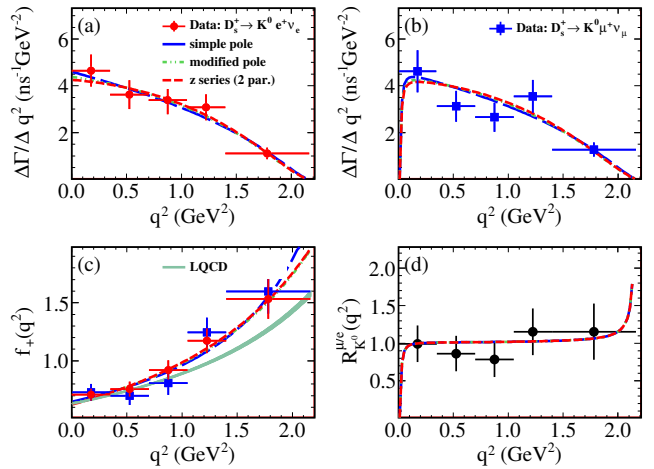


FIG. 3. (Color online) Fits to the partial decay rates for (a) $D_s^+ \rightarrow K^0 e^+ \nu_e$ and (b) $D_s^+ \rightarrow K^0 \mu^+ \nu_\mu$. (c) Projection onto $f_+^{K^0}(q^2)$ for the two SL decays, while the hatched curves show the LQCD prediction in Ref. [7]. (d) The measured $\mathcal{R}_{K^0}^{\mu/e}(q^2)$ in various q^2 intervals. Dots with error bars are data, the curves show fits with various FF parameterizations.

We perform a simultaneous fit to the partial decay rates measured in SL decays $D_s^+ \rightarrow K^0 e^+ \nu_e$ and $D_s^+ \rightarrow K^0 \mu^+ \nu_\mu$, where the two SL decays share the same parameters for the hadronic FF $f_+^{K^0}(q^2)$. Figure 3 show the fits to the partial decay rates and the projections of the FF $f_+^K(q^2)$ for $D_s^+ \rightarrow K^0 e^+ \nu_e$ and $D_s^+ \rightarrow K^0 \mu^+ \nu_\mu$ decays. The numerical results of $f_+^{K^0}(0)|V_{cd}|$ from the χ^2 fit are summarized in Table II. Taking the $|V_{cd}| = 0.22487 \pm 0.00068$ [4] from the CKMfitter as an input, we also measure $f_+^{K^0}(0)$ as summarized in the last column of Table II. The measured FF in $D_s^+ \rightarrow K^0$ transition at $q^2 = 0$ is consistent with 0.6307(20) as predicted by a LQCD calculation [7]. However, the dependence of the measured FF on q^2 shows roughly 2σ deviations with that from the LQCD calculation in the high- q^2 region, as shown in Fig. 4. Comparisons of the measured $f_+^{K^0}(q^2)$ with other theoretical calculations are also shown in Fig. 4.

Combining $\mathcal{B}(D_s^+ \rightarrow K^0 e^+ \nu_e) = (2.98 \pm 0.23_{\text{stat}} \pm 0.12_{\text{syst}}) \times 10^{-3}$ measured in Ref. [6] and $\mathcal{B}(D_s^+ \rightarrow K^0 \mu^+ \nu_\mu) = (2.89 \pm 0.27_{\text{stat}} \pm 0.12_{\text{syst}}) \times 10^{-3}$ measured in this work, we obtain the relative ratio between μ and e modes to be

$$\mathcal{R}_{K^0}^{\mu/e} = 0.97 \pm 0.12_{\text{stat}} \pm 0.04_{\text{syst}},$$

which is consistent with $\mathcal{R}_{K^0}^{\mu/e} = 0.98099(10)^{\text{QCD}}[500]^{\text{QED}}$ from LQCD [7], and the SM predictions in Refs. [8–17]. In addition, we also measured the $\mathcal{R}_{K^0}^{\mu/e}(q^2)$ in various q^2 intervals and the result is shown in Fig. 3 (d), which also consistent with the SM predictions.

To summarize, this Letter reports the first measure-

TABLE II. Hadronic form factors of $D_s^+ \rightarrow K^0 \ell^+ \nu_\ell$, where the first uncertainties are statistical and the second systematic. The correlation coefficient between the two fitted parameters is given in the fourth column. The χ^2/NDOF is the goodness-of-fit and NDOF is the number of degrees of freedom.

Parametrization	$f_+^{K^0}(0) V_{cd} $	Parameter ($M_{\text{pole}}/\alpha/r_1$)	Coefficient	χ^2/NDOF	$f_+^{K^0}(0)$
Simple pole [38]	$0.144 \pm 0.007 \pm 0.001$	$1.725 \pm 0.065 \pm 0.018$	0.74	5.2/8	$0.640 \pm 0.031 \pm 0.005$
Modified pole [38]	$0.140 \pm 0.008 \pm 0.002$	$0.636 \pm 0.198 \pm 0.056$	-0.83	5.6/8	$0.623 \pm 0.036 \pm 0.009$
z series (two par.) [39]	$0.140 \pm 0.008 \pm 0.002$	$-4.000 \pm 1.230 \pm 0.346$	0.87	5.8/8	$0.623 \pm 0.036 \pm 0.009$

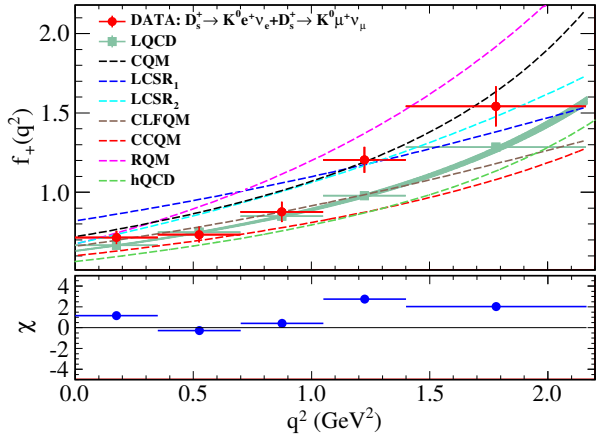


FIG. 4. (Color online) (Upper) Comparisons of $f_+^{K^0}(q^2)$ measured in this work with those calculated from the LQCD [7], CQM [8], LCSR₁ [9], LCSR₂ [10], CLFQM [13], CCQM [15], RQM [17], and the hQCD [18]. (Bottom) Distribution of $\chi = [f_+^{\text{meas}}(q^2) - f_+^{\text{LQCD}}(q^2)] / [\sqrt{\sigma_{f_+^{\text{meas}}(q^2)}^2 + \sigma_{f_+^{\text{LQCD}}(q^2)}^2}]$, calculated with the measured FFs and predicted FFs of the LQCD [7].

ment of the SL decay $D_s^+ \rightarrow K^0 \mu^+ \nu_\mu$. The BF of the decay is measured to be $\mathcal{B}(D_s^+ \rightarrow K^0 \mu^+ \nu_\mu) = (2.89 \pm 0.27_{\text{stat}} \pm 0.12_{\text{syst}}) \times 10^{-3}$. Based on a simultaneous analysis on the decay dynamics in $D_s^+ \rightarrow K^0 \mu^+ \nu_\mu$ and $D_s^+ \rightarrow K^0 e^+ \nu_e$ decays, we report the most precise determination of the FF parameter in the $D_s^+ \rightarrow K^0$ transition and measure $f_+^{K^0}(0) = 0.623 \pm 0.036_{\text{stat}} \pm 0.009_{\text{syst}}$ at $q^2 = 0$ from the z -series expansion. In addition, taking $f_+^{K^0}(0) = 0.6307 \pm 0.0020$ from the LQCD [7] as an input and with $f_+^{K^0}(0)|V_{cd}|$ derived from the z -series expansion, we also obtain $|V_{cd}| = 0.220 \pm 0.013_{\text{stat}} \pm 0.003_{\text{syst}} \pm 0.001_{\text{LQCD}}$. The result shows a comparable precision and is consistent in 1σ with $|V_{cd}| = 0.2330 \pm 0.0029 \pm 0.0133$ [4] from the averaged measurements via $D \rightarrow \pi \ell \nu_\ell$ decays.

The measured BF and FF presented in this work provide a stringent test on various theoretical models. Figures 5 and 6 show the comparisons of the measured BFs, FF and $|V_{cd}|$ with various results in the literature. At a confidence level of 95%, our measured BF disfavors the central values calculated with the CCQM [15, 16] and RQM [17], and the measured FF disfavors the cen-

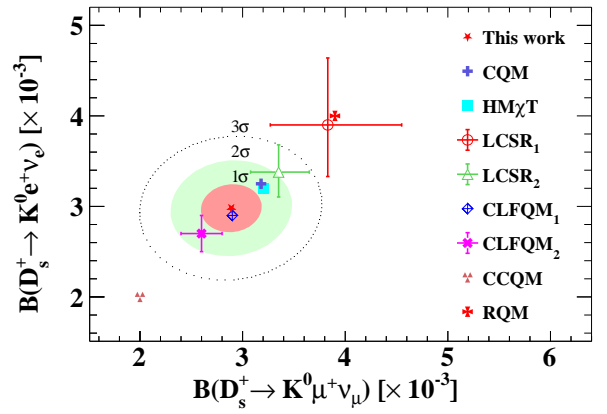


FIG. 5. (Color online) Comparisons of measured BFs for $D_s^+ \rightarrow K^0 e^+ \nu_e$ [6] and $D_s^+ \rightarrow K^0 \mu^+ \nu_\mu$ with various theoretical calculations from the CQM [8], LCSR₁ [9], LCSR₂ [10], HM χ T [11], CLFQM₁ [12], CLFQM₂ [13, 14], CCQM [15, 16], and RQM [17]. The correlation coefficient between the measured BFs is 0.07.

tral value calculated with the CQM [8]. Our result for $|V_{cd}|$ rules out the 2σ tension between the values extracted via $D_s^+ \rightarrow K^0 \ell^+ \nu_\ell$ and that via $D \rightarrow \pi \ell \nu_\ell$ decays [7]. The LFU is also tested with $D_s^+ \rightarrow K^0 \ell^+ \nu_\ell$ in full and separate q^2 intervals, and no LFU violation is found. Combining the $f_+^{K^0}(0)|V_{cd}| = 0.1407 \pm 0.0025$ measured in $D^+ \rightarrow \pi^0 \ell \nu_\ell$ [4] and $f_+^{K^0}(0)|V_{cd}| = 0.140 \pm 0.008_{\text{stat}} \pm 0.002_{\text{syst}}$ measured in this work, we obtain $f_+^{K^0}(0)/f_+^{K^0}(0) = 0.995 \pm 0.061$, which is consistent with LQCD prediction [19–21] and the expectation of U -spin ($d \leftrightarrow s$) symmetry [41]. These measurements provide a unique and rigorous test of the LQCD prediction that the FFs are insensitive to spectator quarks. However, as shown in Fig. 4, our measurements for $f_+^{K^0}(q^2)$ at high- q^2 regions show roughly 2σ tensions with theoretical calculations from the LQCD [7], CLFQM [13], CCQM [15], RQM [17], and the hQCD [18]. The results presented in this Letter provide stringent tests and constraints on various theoretical calculations, especially in QCD theories, and play an important role in understanding the dynamics of charm-hadron SL decays in the non-perturbative region.

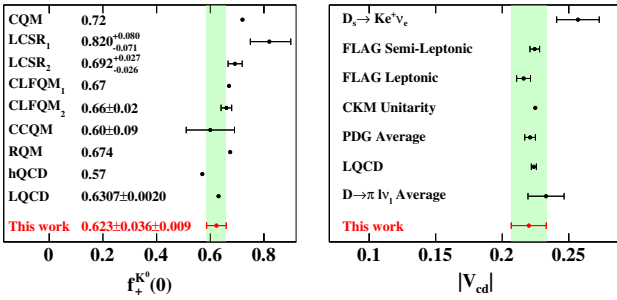


FIG. 6. (Color online) (Left) Comparisons of measured $f_+^{K^0}(0)$ with various theoretical calculations from the CQM [8], LCSR₁ [9], LCSR₂ [10], CLFQM₁ [12], CLFQM₂ [13, 14], CCQM [15, 16], RQM [17], hQCD [18], and the LQCD [7]. (Right) Comparisons of measured $|V_{cd}|$ with various results from $D_s^+ \rightarrow K^0 e^+ \nu_e$ in Ref. [7], FLAG results with $N_f = 2 + 1 + 1$ [40], CKM global fit [4], PDG averaged results [4], LQCD via $D \rightarrow \pi l \nu_e$ decays [7], and averaged measurements via $D \rightarrow \pi l \nu_e$ decays [4].

ACKNOWLEDGMENTS

The BESIII Collaboration thanks the staff of BEPCII (<https://cstr.cn/31109.02.BEPC>) and the IHEP computing center for their strong support. This work is supported in part by National Key R&D Program of China under Contracts Nos. 2023YFA1606000,

2023YFA1606704; National Natural Science Foundation of China (NSFC) under Contracts Nos. 11635010, 11935015, 11935016, 11935018, 12022510, 12025502, 12035009, 12035013, 12061131003, 12192260, 12192261, 12192262, 12192263, 12192264, 12192265, 12221005, 12225509, 12235017, 12361141819, 12375090; the Chinese Academy of Sciences (CAS) Large-Scale Scientific Facility Program; CAS under Contract No. YSBR-101; 100 Talents Program of CAS; The Institute of Nuclear and Particle Physics (INPAC) and Shanghai Key Laboratory for Particle Physics and Cosmology; ERC under Contract No. 758462; German Research Foundation DFG under Contract No. FOR5327; Istituto Nazionale di Fisica Nucleare, Italy; Knut and Alice Wallenberg Foundation under Contracts Nos. 2021.0174, 2021.0299; Ministry of Development of Turkey under Contract No. DPT2006K-120470; National Research Foundation of Korea under Contract No. NRF-2022R1A2C1092335; National Science and Technology fund of Mongolia; Polish National Science Centre under Contract No. 2024/53/B/ST2/00975; STFC (United Kingdom); Swedish Research Council under Contract No. 2019.04595; U. S. Department of Energy under Contract No. DE-FG02-05ER41374. This paper is also supported by the Fundamental Research Funds for the Central Universities, and the Research Funds of Renmin University of China under Contract No. 24XNKJ05.

[1] M. Antonelli *et al.*, *Phys. Rept.* **494**, 197 (2010).
[2] J. D. Richman and P. R. Burchat, *Rev. Mod. Phys.* **67**, 893 (1995).
[3] N. Cabibbo, *Phys. Rev. Lett.* **10**, 531 (1963); M. Kobayashi and T. Maskawa, *Prog. Theor. Phys.* **49**, 652 (1973).
[4] S. Navas *et al.* (Particle Data Group), *Phys. Rev. D* **110**, 030001 (2024).
[5] M. Ablikim *et al.* (BESIII Collaboration), *Phys. Rev. Lett.* **122**, 061801 (2019).
[6] M. Ablikim *et al.* (BESIII Collaboration), *Phys. Rev. D* **110**, 052012 (2024).
[7] A. Bazavov *et al.* (Fermilab lattice and MILC Collaborations), *Phys. Rev. D* **107**, 094516 (2023).
[8] D. Melikhov and B. Stech, *Phys. Rev. D* **62**, 014006 (2000).
[9] Y. L. Wu, M. Zhong and Y. B. Zuo, *Int. J. Mod. Phys. A* **21**, 6125 (2006).
[10] H. J. Tian, Y. L. Yang, D. D. Hu, H. B. Fu, T. Zhang, X. G. Wu, *Phys. Lett. B* **857**, 138975 (2024).
[11] S. Fajfer and J. Kamenik, *Phys. Rev. D* **71**, 014020 (2005).
[12] W. Wang and Y. L. Shen, *Phys. Rev. D* **78**, 054002 (2017).
[13] R. C. Verma, *J. Phys. G* **39**, 025005 (2012).
[14] H. Y. Cheng and X. W. Kang, *Eur. Phys. J. C* **77**, 587 (2017).
[15] N. R. Soni *et al.*, *Phys. Rev. D* **98**, 114031 (2018).
[16] M. A. Ivanov *et al.*, *Front. Phys.* **14**, 64401 (2019).
[17] R. N. Faustov, V. O. Galkin, X. W. Kang, *Phys. Rev. D* **101**, 013004 (2020).
[18] H. A. Ahmed, Y. D. Chen and M. Huang, *Phys. Rev. D* **109**, 026008 (2024).
[19] J. Koponen, C. T. H. Davies and G. Donald [HPQCD Collaboration], arXiv:1208.6242; J. Koponen, C. T. H. Davies, G. C. Donald, E. Follana, G. P. Lepage, H. Na and J. Shigemitsu [HPQCD Collaboration], arXiv:1305.1462.
[20] N. Brambilla *et al.*, *Eur. Phys. J. C* **74**, 2981 (2014).
[21] J. A. Bailey, A. Bazavov, C. Bernard *et al.*, *Phys. Rev. D* **85**, 114502 (2012).
[22] B. C. Ke, J. Koponen, H. B. Li and Y. H. Zheng, *Ann. Rev. Nucl. Part. Sci.* **73**, 285 (2023).
[23] H. B. Li and X. R. Lyu, *Natl. Sci. Rev.* **8**, nwab181 (2021).
[24] X. Leng, X. L. Mu, Z. T. Zou and Y. Li, *Chin. Phys. C* **45**, 063107 (2021).
[25] M. Ablikim *et al.* (BESIII Collaboration), *Nucl. Instrum. Meth. A* **614**, 345 (2010).
[26] C. H. Yu *et al.*, *Proceedings of IPAC2016*, Busan, Korea, 2016.
[27] S. Agostinelli *et al.* (GEANT4 Collaboration), *Nucl. Instrum. Meth. A* **506**, 250 (2003).
[28] S. Jadach, B. F. L. Ward and Z. Was, *Comput. Phys. Commun.* **130**, 260 (2000); *Phys. Rev. D* **63**, 113009 (2001).

- [29] D. J. Lange, *Nucl. Instrum. Meth. A* **462**, 152 (2001); R. G. Ping, *Chin. Phys. C* **32**, 599 (2008).
- [30] J. C. Chen, G. S. Huang, X. R. Qi, D. H. Zhang and Y. S. Zhu, *Phys. Rev. D* **62**, 034003 (2000).
- [31] E. Richter-Was, *Phys. Lett. B* **303**, 163 (1993).
- [32] M. Ablikim *et al.* (BESIII Collaboration), *JHEP* **03** (2025) 197.
- [33] M. Ablikim *et al.* (BESIII Collaboration), *Phys. Rev. Lett.* **135**, 111803 (2025).
- [34] The BFs of $K^0 \rightarrow K_S^0$ and $K_S^0 \rightarrow \pi^+ \pi^-$ are not included in the detection efficiency ϵ_{DT} . The K_S^0 fraction of a K^0 is taken as 50% and the BF of $K_S^0 \rightarrow \pi^+ \pi^-$ is taken from PDG [4].
- [35] M. Ablikim *et al.* (BESIII Collaboration), *Phys. Rev. Lett.* **124**, 241802 (2020).
- [36] M. Ablikim *et al.* (BESIII Collaboration), *Phys. Rev. D* **101**, 112002 (2020).
- [37] There is a slightly difference of $\Gamma_{K^0 e^+ \nu_e}$ reported in this work in comparison to Ref. [6] because the D_s lifetime is updated according to PDG 2024 [4].
- [38] D. Becirevcic and A. B. Kaidalov, *Phys. Lett. B* **478**, 417 (2000).
- [39] T. Becher and R. J. Hill, *Phys. Lett. B* **633**, 61 (2006).
- [40] Y. Aoki *et al.* [Flavour Lattice Averaging Group], arXiv:2411.04268.
- [41] M. Gronau, *Phys. Lett. B* **492**, 297 (2000).